This is a preprint, the final version is subject to change, of the American Mineralogist (MSA)
Cite as Authors (Year) Title. American Mineralogist, in press.
(DOI will not work until issue is live.) DOI: http://dx.doi.org/10.2138/am.2013.4418

Revision 1

The system Na_2CO_3-$MgCO_3$ at 6 GPa and 900-1400 ºC

Anton Shatskiy[1,2*], Pavel N. Gavryushkin [1,2], Igor S. Sharygin[1,2], Konstantin D. Litasov[1,2], Igor N. Kupriyanov[1], Yuji Higo[3], Yuri M. Borzdov[1], Ken-ichi Funakoshi[3], Yuri N. Palyanov[1,2], Eiji Ohtani[4].

[1]V.S. Sobolev Institute of Geology and Mineralogy, Russian Academy of Science, Siberian Branch, Koptyuga pr. 3, Novosibirsk 630090, Russia

[2]Novosibirsk State University, Novosibirsk 630090, Russia

[3]Japan Synchrotron Radiation Research Institute, SPring-8, Kouto, Hyogo 678-5198, Japan

[4]Department of Earth and Planetary Material Science, Tohoku University, Sendai 980-8578, Japan

Abstract

Phase relations in the Na_2CO_3-$MgCO_3$ system have been studied in high-pressure high-temperature (HPHT) multianvil experiments using graphite capsules at 6.0±0.5 GPa pressures and 900-1400 °C temperatures. Sub-solidus assemblages are represented by $Na_2CO_3 + Na_2Mg(CO_3)_2$ and $Na_2Mg(CO_3)_2 + MgCO_3$, with the transition boundary near 50 mol% $MgCO_3$ in the system. The Na_2CO_3-$Na_2Mg(CO_3)_2$ eutectic is established at 1200 ºC and 29 mol% $MgCO_3$. Melting of Na_2CO_3 occurs between 1350 and 1400ºC. We propose that $Na_2Mg(CO_3)_2$ disappears between 1200 and 1250 ºC via congruent melting. Magnesite remains as a liquidus phase above 1300 ºC. Measurable amounts of Mg in Na_2CO_3 suggest an existence of $MgCO_3$

solid-solutions in Na_2CO_3 at given experimental conditions. The maximum $MgCO_3$ solubility in Na-carbonate of about 9 mol% was established at 1100 and 1200 ºC.

The Na_2CO_3 and $Na_2Mg(CO_3)_2$ compounds have been studied using *in situ* X-ray coupled with a DIA-type multianvil apparatus. The studies showed that eitelite is a stable polymorph of $Na_2Mg(CO_3)_2$ at least up to 6.6 GPa and 1000 °C. In contrast, natrite, γ-Na_2CO_3, is not stable at high pressure and is replaced by β-Na_2CO_3. The latter was found to be stable at pressures up to 11.7 GPa at 27 ºC and up to 15.2 GPa at 1200 ºC and temperatures at least up to 800 ºC at 2.5 GPa and up to 1000 °C at 6.4 GPa. The X-ray and Raman study of recovered samples showed that, under ambient conditions, β-Na_2CO_3 transforms back to γ-Na_2CO_3.

Eitelite ($Na_2Mg(CO_3)_2$) would be an important mineral controlling insipient melting in subducting slab and upwelling mantle. At 6 GPa, melting of the $Na_2Mg(CO_3)_2 + MgCO_3$ assemblage can be initiated, either by heating to 1300 ºC under "dry" conditions or at 900-1100 °C under hydrous conditions. Thus, the $Na_2Mg(CO_3)_2$ could control the solidus temperature of the carbonated mantle under "dry" conditions and cause formation of the Na- and Mg-rich carbonatite melts similar to those found as inclusions in olivines from kimberlites and the deepest known mantle rock samples − sheared peridotite xenoliths (190−230 km depth).

Introduction

Previous experimental studies demonstrate that magnesite would be stable at upper and lower mantle conditions and may carry carbon in subducting lithospheric plates into the deep mantle (Fiquet et al., 2002; Katsura and Ito, 1990; Katsura et al., 1991; Litasov et al., 2008; Seto et al., 2008). Occurrences of magnesite as inclusions in diamonds from kimberlites (Bulanova and Pavlova, 1987; Wang et al., 1996) and

ultrahigh pressure metamorphic rocks (Dobrzhinetskaya et al., 2001) exhumed from ≥ 180 km depth (Dobrzhinetskaya et al., 2006; Shatsky et al., 2006; Sobolev and Shatsky, 1990) support these experimental results. Minor amounts of alkalis drastically reduce (by 300-500 ºC) the solidus of magnesite-bearing peridotite and lead to the formation of carbonatite melts (Brey et al., 2011; Litasov et al., 2013). The specific feature of mantle carbonatite melts is high alkali contents, as follows from the study of carbonatite melt inclusions in "fibrous" diamonds (Klein-BenDavid et al., 2009; Navon, 1991; Schrauder and Navon, 1994; Tomlinson et al., 2006; Weiss et al., 2009; Zedgenizov et al., 2004; Zedgenizov et al., 2007) and high-pressure experiments on the partial melting of carbonatites (Litasov et al., 2013), kimberlites (Litasov et al., 2010; Sharygin et al., 2013), carbonated peridotites (Brey et al., 2011), eclogites (Litasov and Ohtani, 2010), and pelites (Grassi and Schmidt, 2011). It is, therefore, essential to know phase relations in simple alkali-alkaline earth carbonate systems under mantle conditions. Particularly, the *T-X* high-pressure phase diagrams of the simple carbonate and carbonate-silicate systems are required for a variety of experimental studies of physicochemical properties of carbonate and carbonate-silicate melts under mantle conditions, namely, measurements of density, element diffusivity, viscosity, wetting, mobility (infiltration and segregation), rheology of the melt impregnated rocks, carbon isotope fractionation etc. As a part of an investigation of those systems, Na_2CO_3-$MgCO_3$ is important, given the abundance of Na in carbonatite melt inclusions in olivines from kimberlites (Kamenetsky et al., 2012; Kamenetsky et al., 2009), sheared peridotite xenoliths (190−230 km depth) (Golovin et al., 2012; Korsakov et al., 2009), and some "fibrous" diamonds (Klein-BenDavid et al., 2004; Klein-BenDavid et al., 2007; Zedgenizov et al., 2011). Since important mantle processes involving carbonates such as kimberlite magma generation, mantle

metasomatism and diamond formation have been occurred at the base of lithospheric mantle (150-230 km depths); 6 GPa and 900-1400 °C are relevant experimental conditions to study binary carbonate systems.

Although the Na_2CO_3-$MgCO_3$ system has not been previously studied, the data on phase relations in more complex systems $K_2Ca(CO_3)_2$-$Na_2Mg(CO_3)_2$ and Na_2CO_3-MgF_2 at 0.1 GPa pressure have been reported (McKie, 1990; Mitchell and Kjarsgaard, 2011). These studies showed that eitelite, $Na_2Mg(CO_3)_2$, is stable in sub-solidus assemblages below 550 ºC in both systems. The melting point of eitelite has been determined by Eitel and Skaliks (1929) as 677 ºC at 0.124 GPa. In this paper, we present experimental data on phase relations in the system Na_2CO_3-$MgCO_3$ at 6 GPa and 900-1400 ºC under nominally "dry" and hydrous conditions and highlight our results of *in situ* X-ray diffraction of Na_2CO_3 and $Na_2Mg(CO_3)_2$ compound at high pressure.

Experimental methods

In this study we conduct three sets of HP-HT multianvil experiments: Kawai experiments to study phase relations in the Na_2CO_3-$MgCO_3$ system using DIA- and wedge-type presses at Tohoku University (Sendai, Japan); BARS (a transliteration of a Russian abbreviation of a pressless split-sphere apparatus) experiments in Na_2CO_3-hydromagnesite join to examine water effect on phase relations in Na-Mg carbonate system using pressless multianvil apparatuses at the V.S. Sobolev IGM SB RAS (Novosibirsk, Russia) (Palyanov et al., 2010; Shatskiy et al., 2011); and X-ray diffraction (XRD) experiments to identify the Na_2CO_3 and $Na_2Mg(CO_3)_2$ crystal structures *in situ* at HPHT conditions using DIA-type presses at the BL04B1 beamline at the SPring-8 synchrotron radiation facility (Hyogo, Japan). All experiments were

performed using graphite sample capsules, which are conventionally employed to seal alkali-carbonate melts in long duration experiments (up to 20-40 hours) under 5.5-6.5 GPa pressures and temperatures up to 1650 ºC (Kanda et al., 1990; Shatskii et al., 2002). The experimental methods employed in the present study were the same as in our resent manuscripts (Shatskiy et al., Under review-a; Shatskiy et al., Accepted). Mixtures of synthetic K_2CO_3 and natural magnesite from Bahia, Brazil, with a composition of $Mg_{0.975}Fe_{0.015}Mn_{0.006}Ca_{0.004}CO_3$ and mixtures of K_2CO_3 and synthetic hydromagnesite, $Mg_5(CO_3)_4(OH)_2 \cdot 4H_2O$ were used as starting materials (Table 1 and 2). Details of pressure and temperature calibration of BARS are given in (Shatskii et al., 2002; Sokol et al., 2007). In this section, we will only focus on peculiarities of measurement of chemical composition of carbonate phases in the Na_2CO_3-$MgCO_3$ system using energy dispersive X-ray scan (EDS) and details of sample characterization by the Raman spectroscopy.

Samples were studied using a JSM 5410 scanning electron microscope equipped with Oxford Instruments Link ISIS Series 300 energy-dispersive X-ray spectrometer (EDS) at Tohoku University (Sendai, Japan). The EDS spectra were collected by rastering the electron beam over a surface area available for the analysis with linear dimensions from 10 to 300 μm at 15 kV accelerating voltage and 10 nA beam current. No beam damage or change in measured composition with time was observed at the current setting used. The EDS was calibrated at the same conditions by rastering the electron beam over a sample cross-section area, up to 0.5-0.8 mm in linear dimensions. For that purpose, we employed post-experimental samples with known compositions and a homogeneous texture synthesized well below eutectic temperatures or quenched from super-liquidus charges. To correct EDS data of quenched melt in the system Na_2CO_3-hydromagnesite, we performed additional calibration using samples with

complete melting in this system. We also confirmed that the size of the analyzed region has no effect on the resulting data, as long as the area is significantly larger than the grains. In our previous studies on the K-Mg and K-Ca binary carbonate systems, the deviation of K/Mg ratio measured by EDS from the actual sample composition generally did not exceed a confidence limit of our EDS measurements (~ 0.5 mol%). Yet, in present study, we found significant deficit of Na relative to the actual composition. The deficit systematically increases from the end member (Na_2CO_3 and $MgCO_3$) sides toward the near intermediate composition, where the Na_2CO_3 deficit is in order of 10 mol%. Results of calibration are shown in Figure 1. The best fit of the data is described by following polynomial expressions for the Na_2CO_3-$MgCO_3$ system:

$$k = 0.78469 + 0.03733 \times X - 1.0712 \times 10^{-3} \times X^2 + 1.26334 \times 10^{-5} \times X^3 - 5.59045 \times 10^{-8} \times X^4,$$

and for the Na_2CO_3-hydromagnesite system:

$$k = 0.36301 + 0.0582 \times X - 0.001 \times X^2 + 0.000004925 \times X^3,$$

where X is the measured content of Na_2CO_3.

Raman measurements were performed using a Horiba J.Y. LabRAM HR800 Raman microspectrometer with the 514 nm line of an Ar-ion laser at the V.S. Sobolev IGM SB RAS (Novosibirsk, Russia). Spectra were recorded at room temperature in backscattering geometry with the laser power of about 1 mW and spectral resolution of approximately 2 cm^{-1}. To prevent the reaction of the carbonates with air, the samples were placed into a Linkam FTIR 600 stage, which was purged with dry argon. A 50×/0.50 long working distance objective was used to focus the laser beam onto the sample and to collect Raman signal.

Experimental results

The system Na_2CO_3-$MgCO_3$. Selected backscattered electron (BSE) images of sample cross-sections in the system Na_2CO_3-$MgCO_3$ are shown in Figure 2. The sub-solidus samples were represented by homogeneous aggregates of carbonate phases, with grain size varying from several micrometers to several tens of micrometers (Fig. 2e,g-j). In non-stoichiometric mixtures, the limited reagents, i.e. $MgCO_3$ at $X(Na_2CO_3) > 50$ mol% (Fig. 2g,j) and Na_2CO_3 at $X(Na_2CO_3) < 50$ mol% (Fig. 2e), have been consumed completely (Table 1). In stoichiometric mixture, $X(Na_2CO_3) = 50$ mol%, both reagents, Na_2CO_3 and $MgCO_3$, were completely consumed to form $Na_2Mg(CO_3)_2$ at 1100 and 1200 ºC (Table 1), while a few relicts of Na_2CO_3 and $MgCO_3$ remained at 900 and 1000 ºC (Fig. 2h,i, Table 1). This suggests that reactions have typically gone to completion and equilibrium has been achieved.

A dome-shaped volume of carbonate crystals up to 100 μm in size in the cool region and a quenched melt segregated to the hot region were observed in the run products below liquidus (Fig. 2a-d,f,k,l). The liquid-crystal interface coinciding with the typical shape expected for an isotherm in a sample charge with maximum radial and axial thermal gradients of about 5 and 10°C/mm (Shatskiy et al., Accepted). The melts quenched from 1400 to 200ºC with a rate of about 60°C/sec, were represented by dendritic aggregates rather than glass. The liquid-crystal interface has a rounded outline coinciding with an ordinary shape of the isotherm in a high-pressure cell (Fig. 2a-c).

Phase relations established in the system Na_2CO_3-$MgCO_3$ at 6 GPa are illustrated in Figure 3. An intermediate phase, $Na_2Mg(CO_3)_2$, was observed between 900 and 1200ºC, in association with Na_2CO_3 in the range of 10 – 40 mol% $MgCO_3$ (Fig. 2d,g,j,k) and in association with magnesite in the range of 60 – 90 mol% $MgCO_3$ (Fig. 2e). First melt with nearly eutectic composition (~29 mol% $MgCO_3$) appeared at

1200ºC at $X(Na_2CO_3)$ > 50 mol% (Fig. 2d), whereas at $X(Na_2CO_3)$ < 50 mol%, melt was established at 1250ºC (Fig. 2i).

The Na_2CO_3 and $Na_2Mg(CO_3)_2$ compounds enter their sub-liquidus phases below and above 25 mol% $MgCO_3$ in the system, respectively (Fig. 2d,k,l, 3). As can be seen in Table 1, the Na_2CO_3 solid-solution containing about 95 mol% $MgCO_3$ was observed at 1300 ºC. We also found that pure Na_2CO_3 remains solid at 1350 ºC and melts at 1400 °C (Shatskiy et al., Under review-b). The established melting temperature is about 500 ºC higher than that at ambient pressure. Measurable amounts of Mg in Na_2CO_3 suggest an existence of $MgCO_3$ solid solutions in Na_2CO_3 at given experimental conditions (Fig. 3, Table 1). The maximum $MgCO_3$ solubility in Na-carbonate of about 9 mol% was established at 1100 and 1200 ºC.

Magnesite, whose melting temperature exceeds 1800ºC at 6 GPa (Katsura and Ito, 1990), was observed as a sub-liquidus phase at 1250, 1300 and 1400 ºC and $X(Na_2CO_3)$ < 50 mol%. Na solubility in magnesite does not exceed the detection limit of EDS employed in our study (i.e. <0.5 mol% Na_2CO_3) (Table 1). Therefore, it is concluded that there is very little, if any, solid solution of Na_2CO_3 in the $MgCO_3$ at 6 GPa.

The $Na_2Mg(CO_3)_2$ remains in its solid phase at 1200 ºC and disappears at 1250ºC (Fig. 3). The established melting temperature is about 550 ºC higher than that at 0.124 GPa reported by (Eitel and Skaliks, 1929).

The system Na_2CO_3-hydromagnesite. Phase relations established in the system Na_2CO_3-hydromagnesite at 6 GPa are illustrated in Figures 4 and 5 and summarized in Table 2. Below, we use $X(MgCO_3) = MgCO_3/(MgCO_3+Na_2CO_3)$ molar ratio to show system composition instead of *X*(hydromagnesite) = hydromagnesite /(hydromagnesite +Na_2CO_3) ratio for clarity. Consecutive increase of hydromagnesite

content in the system at 900 ºC leads to a change in the phase composition from Na_2CO_3 + liquid at $7 \leq X(MgCO_3) \leq 19$ mol% to $Na_2Mg(CO_3)_2$ + liquid at $33 \leq X(MgCO_3) \leq 42$ mol% and magnesite + liquid/fluid at $52 \leq X(MgCO_3) \leq 87$ mol%. Rise in temperature to 1000 and 1100 °C causes disappearance of $Na_2Mg(CO_3)_2$ compound and expands the range of complete melting to $19 \leq X(MgCO_3) \leq 42$ mol% and $19 \leq X(MgCO_3) \leq 63$ mol% in the entire compositional range. The obtained diagram shows that increase in water content in the system at constant $Na_2CO_3/MgCO_3$ ratio in a substrate shifts the coexisting melt composition toward Na-poor hydrous-rich melt/fluid (Fig. 5). A similar correlation was reported for compositional co-variations of Na_2O and H_2O among kimberlites from Siberia and Canada (Kamenetsky et al., 2009).

The Na_2CO_3 melt is known as a solvent catalyst for the graphite-to-diamond transformation under anhydrous and hydrous conditions (Akaishi et al., 1990; Kanda et al., 1990; Pal'yanov et al., 2002; Sokol et al., 1998). Although our experiments were performed in the field of the thermodynamic stability of diamond (Kennedy and Kennedy, 1976), no diamonds were found in the run products, even after sample annealing at 1400 ºC and 6 GPa for 6 hours. This is consistent with previous results for the system Na_2CO_3-C, in which diamond appeared only after 40 hours at 5.7 GPa and 1360 °C (Pal'yanov et al., 1999b). This can be explained by a long induction period of diamond nucleation in the Na_2CO_3 carbonate systems, which diminishes with increasing temperature and pressure from ~40 hours at 5.7 GPa and 1360 ºC to 20 minutes at 7 GPa and 1700-1750 ºC (Pal'yanov et al., 1999a).

The structure of Na_2CO_3. Several temperature-induced phase transitions in Na_2CO_3 were established experimentally by means of *in situ* X-ray diffraction studies at ambient pressure (Table 3). On the other hand, no pressure-induced phase

transitions are expected up to 11.3-17.7 GPa at room temperature, based on the *ab* initio calculations (Cancarevic et al., 2006). The results of our *in situ* XRD study of Na_2CO_3 under HP-HT conditions are illustrated in Figures 6 and 7. As can be seen, the temperature range of the stability field of β-Na_2CO_3 expands with pressure from 150 ºC up to 1000 °C or more at 6 GPa. γ-Na_2CO_3 was observed only under ambient conditions after decompression. β-Na_2CO_3 does not transform to α-Na_2CO_3 at least up to 800 ºC at 2.5 GPa and up to 1000 °C at 6.4 GPa. We did not observe any pressure-induced phase transitions in β-Na_2CO_3 up to 11.7 GPa at 27 ºC and up to 15.2 GPa at 1200 ºC, which is consistent with the theoretical prediction of Cancarevic et al. (2006). Obtained crystal lattice parameters of β-Na_2CO_3 are shown in Table 4.

The structure of $Na_2Mg(CO_3)_2$. The structure of $Na_2Mg(CO_3)_2$ compound has previously been determined at ambient conditions by means of X-ray diffraction study of single crystals synthesized at 1 atm and 74 °C. The study reveals that this compound, eitelite, has rhombohedral $R\bar{3}$ structure, with one molecular formula per unit cell (Pabst, 1973). In the present study, we collected several energy dispersive XRD patterns from the Na_2CO_3-$MgCO_3$ stoichiometric mixture during sample heating to 1000°C at about 6.5 GPa, further cooling and decompression at room temperature down to 1 atmosphere. The experimental P-T pathway is shown in Figures 8. The first XRD pattern was taken at 500 ºC and 6.3 GPa after 70 min sample annealing exhibits peaks of eitelite, magnesite, and β-Na_2CO_3. Further sample annealing at 800 ºC and 6.5 GPa for 35 min substantially diminishes the intensity of magnesite and β-Na_2CO_3 peaks, which finally disappear at 1000 ºC and 6.6 GPa (Fig. 9a). Hence, $Na_2Mg(CO_3)_2$ rather than the Na_2CO_3 + $MgCO_3$ assemblage remains stable at $X(Na_2CO_3)$ = 50 mol% below 1000 °C.

As can be seen, no significant change in XRD patterns occurred during further sample cooling and decompression down to ambient conditions (Fig. 9b,c). Thus, eitelite is a stable polymorph of $Na_2Mg(CO_3)_2$, at least up to 6.6 GPa and 1000 °C. Obtained crystal lattice parameters of eitelite along the PT-path are shown in Table 5.

Raman spectra of γ-Na_2CO_3 and $Na_2Mg(CO_3)_2$.

The Raman spectroscopy is an indispensable tool for the identification of the submicron specimens especially compounds with strong covalent bonds, such as carbonates and sulfates. Since this method is widely applicable for the study of mantle-derived alkali-rich carbonatite melt inclusions (Kaminsky et al., 2009; Korsakov et al., 2009; Sharygin et al., Accepted) and for the identification of minor phases in carbonate-silicate systems, the obtained carbonate phases were characterized by Raman spectroscopy.

We collected several Raman spectra from Na_2CO_3 recovered from experiments at 1100, 1200, and 1300 °C. The obtained spectra correspond to the γ-modification of Na_2CO_3 (Fig. 10a). The most intense Raman bands at 1079 and 1082 cm^{-1} were assigned to the ν_1 symmetric stretching mode of the carbonate-ion. The low intensity band at 1431 cm^{-1} may be ascribed to the ν_3 normal mode, and the band near 699 cm^{-1} is attributed to the ν_4 symmetric bending mode (Meekes et al., 1986). The spectra also revealed three bands at 90 cm^{-1}, 149 cm^{-1}, and 189 cm^{-1}, which may be assigned to the external vibration modes between the cation and anion group. An additional band at 1104 cm^{-1} would be related to the $Na_2Mg(CO_3)_2$, which exsolved from the $MgCO_3$ solid solution in Na_2CO_3.

The Raman spectra of $Na_2Mg(CO_3)_2$ recovered from experiments at 6 GPa and 900-1200 °C coincide with the spectrum of eitelite (Fig. 12.14 in (White, 1974)) synthesized at 1 atm and 74 °C according to the method described by Pabst (1973).

The spectrum has a single, strong band at 1105 cm^{-1}, which can be attributed to the CO_3^{-2} symmetric stretching mode (Fig. 10b). Weaker bands at 208 and 263 cm^{-1} are due to lattice vibration. A very intense lattice mode at 91 cm^{-1} may be due to the motion of the highly polarizable Na ion (White, 1974).

Discussion

Originally, eitelite is known as a mineral from ambient pressure mineralization. However, eitelite was recently reported as a daughter phase in fluid/melt inclusions in Cr-spinel and olivine from the hypabyssal kimberlites of the Koala pipe, Canada (Kamenetsky et al., 2012), "fibrous" diamonds from Panda kimberlite diatreme, Canada (Smith et al., 2011) and in olivine from the sheared peridotite xenoliths from Udachnaya-East kimberlite pipe, Russia (Sharygin et al., Accepted). Moreover, our experimental data suggest that eitelite would be stable down to the mantle depth of 200 km. Yet, a comparison of an experimentally measured melting points of eitelite, near 1250 °C at 6 GPa and 677 ºC at 0.124 GPa (Eitel and Skaliks, 1929) and the possible P-T pathway of ascent of kimberlite magma (Kavanagh and Sparks, 2009), wherein temperature drops from 1410 °C at 6 GPa to 1270 at about 1 GPa, clearly indicate that eitelite should unavoidably melt during upward transport. Thus, the eitelite found as inclusions in mantle minerals has been precipitated from trapped melts at hypabyssal conditions, rather than represents original mantle mineralization.

Although eitelite could barely survive adiabatic ascent, the eutectic temperature of magnesite-eitelite assemblage is large enough to allow transport to the deep upper mantle in subducting lithospheric slab. Therefore, eitelite would be an important mineral controlling insipient melting in subducting slab. At 6 GPa, melting of the $Na_2Mg(CO_3)_2 + MgCO_3$ assemblage can be initiated, either by heating to 1250 ºC

under "dry" conditions or by adding a certain amount of water at 900-1100 °C. Thus, the $Na_2Mg(CO_3)_2$ could control the solidus temperature of the carbonated mantle under "dry" conditions and cause formation of the Na- and Mg-rich carbonatite melts, similar to those found as inclusions in olivines from kimberlites (Kamenetsky et al., 2009) and the deepest known mantle rock samples − sheared peridotite xenoliths (190−230 km depth) (Golovin et al., 2012; Korsakov et al., 2009).

The binary alkali-alkaline earth carbonates with similar stoichiometry $(K,Na)_2(Ca,Mg)(CO_3)_2$, were found to be stable at 6 GPa in the K_2CO_3-$MgCO_3$ system at 900-1200 °C (Shatskiy et al., Accepted), in the K_2CO_3-$CaCO_3$ system at 900 °C (Shatskiy et al., Under review-a) and in the K/Na_2CO_3-$CaMg(CO_3)_2$ systems at 900-1200/1100 °C (Shatskiy et al. in preparation). The K-Mg-rich end member was also established in the K-rich carbonated peridotite (K/Na = 15, (Mg+Fe)/Ca = 17 and SiO_2/CO_2 = 3.2) at 10 GPa and 1400 °C (Brey et al., 2011) and in the K-bearing dolomitic carbonatite (K/Na = 2.3, (Mg+Fe)/Ca = 1.5 and SiO_2/CO_2 = 0.07) at pressures to 21 GPa and temperatures to 1450 °C (Litasov et al., 2013). Nevertheless, the eitelite stability in complex carbonate-silicate systems has not been reported under mantle conditions. Furthermore, $Na_2Mg_2(CO_3)_3$, $Na_2Ca_2(CO_3)_3$, $K_2Mg(CO_3)_2$, $(K,Na)_2Ca_4(CO_3)_5$ Na-$CaCO_3$ and $MgCO_3$ carbonates rather than eitelite have been established in Na-bearing dolomitic carbonatite (K/Na = 0.2, (Mg+Fe)/Ca = 0.8 and SiO_2/CO_2 = 0.07) (Litasov et al., 2013). However, this does not exclude eitelite stability in the specific Na-Mg-rich carbonate-silicate environments.

Since carbonate would be the major contributors to the incipient melting in the oxidized mantle domains under anhydrous conditions, it is interesting to discuss an effect of their cation composition on the solidus temperature of the carbonate and carbonate-silicate systems. According to experiments at 6 GPa, addition of $CaCO_3$ in

the magnesium carbonate and carbonate-silicate systems depresses their melting/solidus temperatures by 370 and 460 °C, respectively: $T_{Melting}(MgCO_3)$ = 1810 °C (Katsura and Ito, 1990), $T_{Melting}$ ($CaMg(CO_3)_2$) = 1350 °C (Buob et al., 2006), $T_{Solidus}(MgO\text{-}SiO_2\text{-}CO_2)$ = 1750 °C (Katsura and Ito, 1990), $T_{Solidus}$ ($MgO\text{-}CaO\text{-}SiO_2\text{-}CO_2$) = 1430 °C (Luth, 2006), $T_{Solidus}$ ($MgO\text{-}CaO\text{-}Al_2O_3\text{-}SiO_2\text{-}CO_2$) = 1380 °C (Dalton and Presnall, 1998). On the basis of our data on the Na_2CO_3-$MgCO_3$ and K_2CO_3-$MgCO_3$ systems (Shatskiy et al., Accepted), the presence of alkalis initiates melting at 1200-1250 °C at 6 GPa. Compared to the eutectics determined in the K/Na-Mg carbonates, the solidi of K-bearing carbonated peridotite ($T_{Solodus} \leq$ 1100 °C at 6 GPa) (Brey et al., 2011) and Na-bearing carbonated eclogite ($T_{Solodus}$ = 1000 °C at 6.5 GPa) (Hammouda, 2003) are at lower temperatures. This difference undoubtedly reflects the influence of additional constituents, such as CaO. Indeed, melting in the K/Na_2CO_3-$CaMg(CO_3)_2$ systems was established at 1000 and 1100 °C, respectively (Shatskiy et al. in preparation).

Acknowledgements

We thank R. W. Luth and K. Kiseeva for thorough reviews and suggestions and J. Kung and K. Putirka for editorial handling and comments. The synchrotron radiation experiments were performed at the BL04B1 in SPring-8 with the approval of the Japan Synchrotron Radiation Research Institute (JASRI) (proposals 2010B1308, 2011B1416, 2011B1163, and 2012B1548). This study was conducted as a part of the Global Center-of-Excellence program at Tohoku University. This work was also supported by the Ministry of education and science of Russia (project No. 14.B37.21.0601) and by the Russian Foundation for Basic Research (project Nos. 12-05-01167 and 12-05-33008).

Table 1. Compositions (in mol% Na_2CO_3) of the run products in the system Na_2CO_3-$MgCO_3$ at 6 GPa.

Run,		$X(Na_2CO_3)$ in the system, mol%							
T, τ	Phase	90	75	60	50	40	30	20	10
ES346	Na_2CO_3	–[a]	×	×	×	–	–	–	–
1400ºC	$Na_2Mg(CO_3)_2$	–	×	×	×	–	–	–	–
6 h	$MgCO_3$	–	×	×	×	0.5	0.4	0.5	0.5
	MgO	–	×	×	×	0.1*	0.2*	–	–
	Liquid	100.0	×	×	×	45.8(2)	42.8(6)	45.4(3)	39.6(4)
T2020	Na_2CO_3	94.9(1.4)	–	–	–	–	–	–	–
1300ºC	$Na_2Mg(CO_3)_2$	–	–	–	–	–	–	–	–
4 h	$MgCO_3$	–	–	–	–	0.0	0.2	0.3	0.1
	Liquid	87.5(6)	+	59.4(5)	54.5	47.5(5)	48.3	44.7(8)	45.0
T2024	Na_2CO_3	×	–	–	–	×	×	–	–
1250ºC	$Na_2Mg(CO_3)_2$	×	–	–	–	×	×	–	–
10 h	$MgCO_3$	×	–	–	–	×	×	0.3	0.1
	Liquid	×	73.8	61.9(1)	49.4(3)	×	×	+	46.0
ES342	Na_2CO_3	90.7(3)	90.6(2)	90.8	–	–	–	–	–
1200ºC	$Na_2Mg(CO_3)_2$	50.1	50.1	50.0	49.7	51.3	50.3	49.4	50.0
12 h	$MgCO_3$	–	–	–	–	0.0	0.4	0.4	0.2
	Liquid	71.2(1.8)	+	+	–	–	–	–	–
T2022	Na_2CO_3	90.6(4)	90.9(1)	90.6(4)	–	–	–	–	–
1100ºC	$Na_2Mg(CO_3)_2$	48.9(1.4)	49.9	51.3	50.3	49.7	47.8	50.0	49.5
16 h	$MgCO_3$	–	–	–	–	n.d.	0.5	0.1	-0.1
	Liquid	–	–	–	–	–	–	–	–
ES343	Na_2CO_3	93.3(2.2)	94.2	×	92.5(3.4)	–	×	×	–
1000ºC	$Na_2Mg(CO_3)_2$	49.7	51.6	×	46.6	49.8	×	×	50.6
19 h	$MgCO_3$	–	–	×	0.2	0.3	×	×	0.4
	Liquid	–	–	×	–	–	×	×	–
T2021	Na_2CO_3	96.4(2)	96.7(1.3)	×	96.0(5)	–	–	×	–
900ºC	$Na_2Mg(CO_3)_2$	53.5	50.0	×	50.4	49.4	48.9	×	48.8(8)
43 h	$MgCO_3$	–	–	×	0.4	n.d.	0.2	×	0.3(1)
	Liquid	–	–	×	–	–	–	×	–

Note: [a] – It is pure Na_2CO_3 system; τ – run duration; × – no data. Standard deviations are given in parentheses, where the number of measurement is more than one. Letters in the run number, ES and T denote the type of press, wedge and DIA, respectively. * - Na_2O content in periclase (in mol%). n.d. – not determined.

Table 2. Conditions and results of experiments in the system Na_2CO_3-hydromagnesite at 6 GPa.

Run		Initial compositions, $MgCO_3/Na_2CO_3/H_2O$, mol%							
T, τ	Phases	7/89/4	17/73/10	28/57/15	34/47/19	40/37/23	46/28/26	53/18/29	58/9/33
1486/2, 1100°C, 15 h.	Na_2CO_3[a]	94.9(6)	–	–	–	–	–	–	–
	$MgCO_3$[a]	–	–	–	–	–	–	0.3(2)	0.4(0)
Liquid	Mole fract.	0.85(3)	1	1	1	1	1	0.93(1)	0.70(7)
	$MgCO_3$	7.5(1)	+	+	+	+	+	50.7(4)	49.6(2.4)
	Na_2CO_3	87.8(3)	+	+	+	+	+	18.9(1)	10.9(5)
	H_2O	4.7(2)	+	+	+	+	+	30.4(2)	39.5(1.8)
1002/1, 1000°C, 30 h.	Na_2CO_3[a]	93.2(3)	–	–	–	–	–	–	–
	$MgCO_3$[a]	–	–	–	–	0.5(1)	0.5(0)	0.5(0)	0.5(2)
Liquid	Mole fract.	0.33(9)	1	1	1	0.95(4)	0.77(5)	0.65(1)	0.55(10)
	$MgCO_3$	7.8(5)	+	+	+	39.1(9)	40.1(1.6)	41.8(5)	43.6(5.0)
	Na_2CO_3	80.2(6)	+	+	+	38.0(6)	30.9(8)	22.3(2)	12.2(1.1)
	H_2O	12.0(5.5)	+	+	+	22.9(3)	29.0(8)	35.9(3)	44.2(3.9)
1001/1, 900°C, 38 h.	Na_2CO_3[a]	93.3(9)	93.9(8)	–	–	–	–	–	–
	$Na_2Mg(CO_3)_2$[a]	–	–	50.3(3)	50.4(1)	–	–	–	–
	$MgCO_3$[a]	–	–	–	–	0.3	0.6	0.1	0.2
Liquid	Mole fract.	0.22(7)	0.70(7)	0.75(3)	0.8(3)	0.85(6)	0.73(10)	0.52(1)	0.38(16)
	$MgCO_3$	18.2(2.9)	22.4(1.5)	23.9(6)	31.4(5)	36.4(1.6)	38.8(3.5)	36.5(3)	34.8(7.7)
	Na_2CO_3	63.7(4.4)	63.6(2.7)	58.3(2)	46.6(1)	39.6(1.0)	31.6(1.8)	24.3(1)	14.1(1.7)
	H_2O	18.1(7.3)	13.9(1.2)	17.8(4)	21.9(6)	23.9(6)	29.7(1.7)	39.2(2)	51.1(6.1)

Note: [a] – composition is given in mol% Na_2CO_3; (–) – no phase; × – no data; τ – run duration. Standard deviations are given in parentheses, wherever the number of measurement is more than one. CO_2 and H_2O contents in the liquid were calculated from mass balance using the compositions of starting material and analyses of phases.

Table 3. Phases of Na_2CO_3 at 1 atm. T_s (°C) is stability field.

Phase	T_s (°C)	Structure	T (°C)	Cell parameters (Å, º)				Reference
α	481-?	$P6_3/mmc$	483	9.02	5.21	6.45	90	(Swainson et al., 1995)
β	332-481	$C2/m$	332	8.98	5.25	6.21	99.33	(Swainson et al., 1995)
γ	-103-360	$C2/m(\alpha 0\gamma)0s$	22	8.92	5.25	6.05	101.35	(Dusek et al., 2003)

Table 4. Lattice parameters of β-Na_2CO_3.

P, GPa*	*T, ºC*	*a*	*b*	*c*	*β*	*V*
6.44(14)	1000	8.9562(8)	5.2626(7)	6.3355(7)	96.595(8)	296.64(4)
15.20(6)	1200	8.941(1)	5.1664(4)	6.238(1)	96.01(2)	286.62(5)
4.62(7)	200	8.831(2)	5.1884(4)	6.292(1)	97.57(2)	285.79(5)
9.32(13)	27	8.547(2)	5.12242(4)	6.367(1)	99.53(1)	274.93(4)
6.20(11)	27	8.661(2)	5.0806(3)	6.181(1)	97.89(1)	269.44(4)
4.78(10)	27	8.530(2)	5.1867(3)	6.410(1)	99.97(1)	279.33(4)
3.41(13)	27	8.554(2)	5.2055(3)	6.463(1)	100.24(1)	283.20(4)

Note: * - Au pressure scale (Anderson et al., 1989).

Table 5. Lattice parameters of eitelite, $Na_2Mg(CO_3)_2$.

P, GPa*	*T, ºC*	*a*	*c*	*V*
6.32(3)	500	4.8776(2)	15.802(2)	325.56(3)
6.52(4)	800	4.9134(2)	15.957(2)	333.62(4)
6.62(5)	1000	4.9253(3)	16.078(2)	337.78(4)
6.30(2)	900	4.9240(3)	16.043(2)	336.87(4)
5.59(5)	800	4.9192(3)	16.008(2)	335.45(4)
4.52(9)	27	4.8678(2)	15.814(2)	324.51(3)
3.12(6)	27	4.8832(2)	15.917(2)	328.71(3)
1.34(4)	27	4.9107(2)	16.051(2)	335.21(3)
0.95(9)	27	4.9076(2)	16.125(2)	336.33(4)
0.00(1)	27	4.9424(2)	16.300(2)	344.83(4)

Note: * - MgO pressure scale (Jamieson et al., 1982).

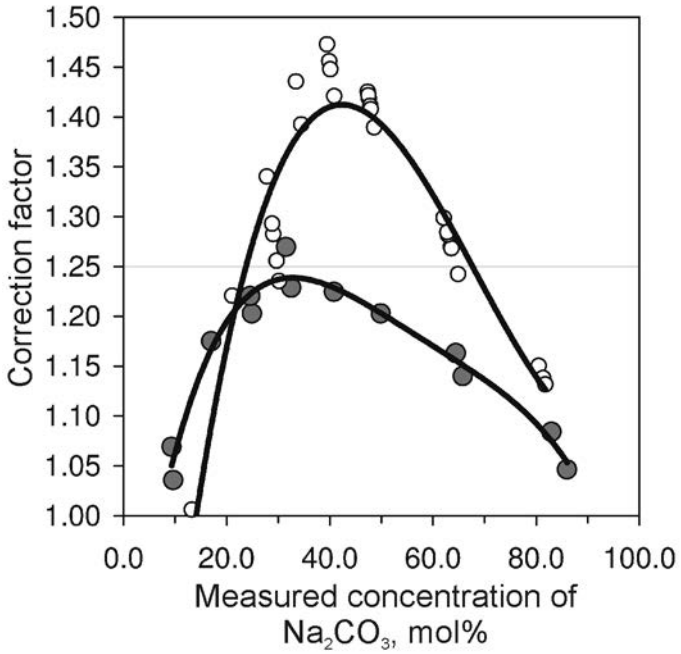

Figure 1. Correction factor, $k = X_0/X$, vs. measured concentration of Na_2CO_3, X, in mol% for the system Na_2CO_3-$MgCO_3$, grey circles, and for the system Na_2CO_3-hydromagnesite, opened circles.

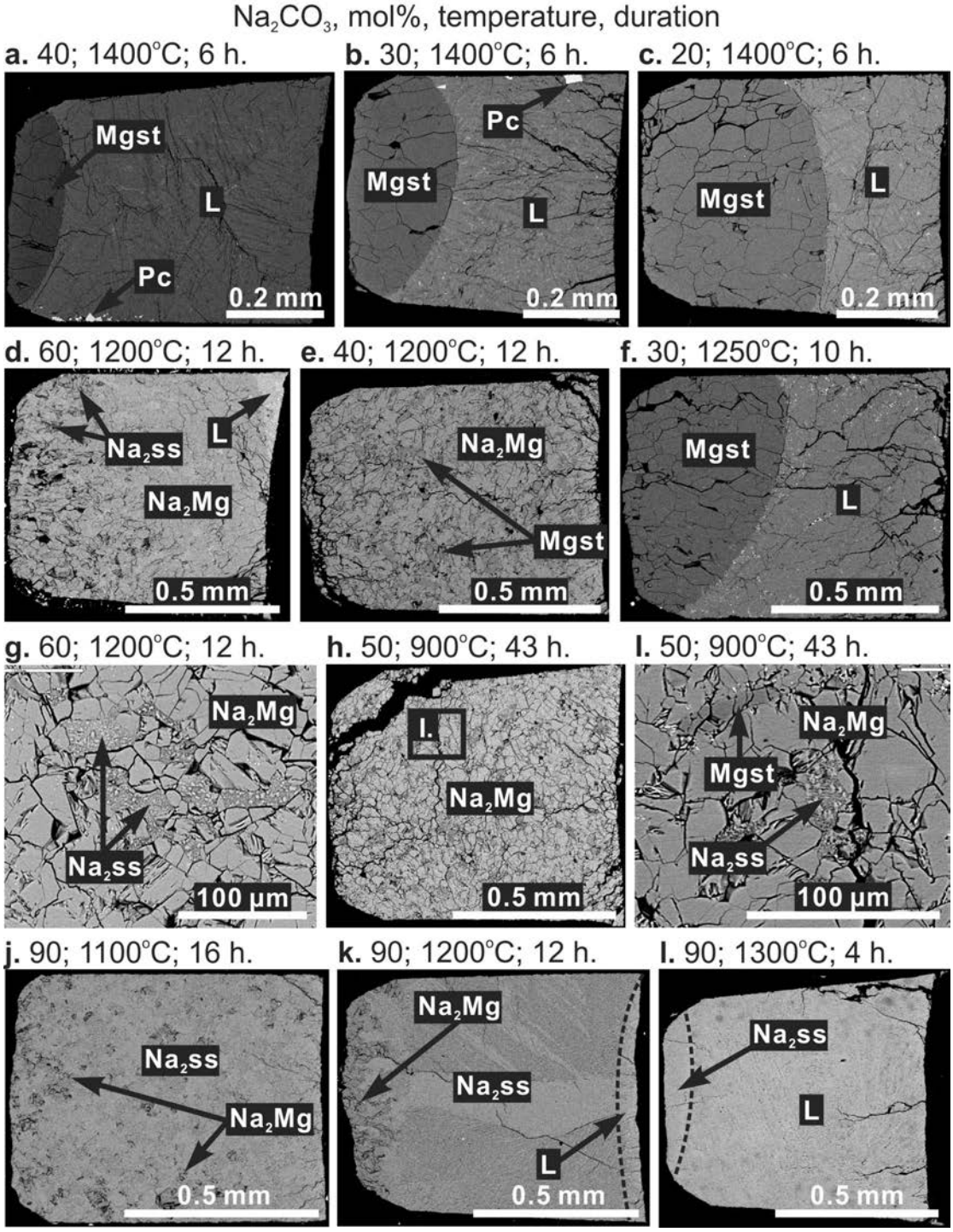

Figure 2. Representative BSE images of sample cross-sections illustrating phase relations in the systems Na_2CO_3-$MgCO_3$ at 6 GPa. Na_2ss = $MgCO_3$ solid solution in Na_2CO_3; Na_2Mg = $Na_2Mg(CO_3)_2$; Mgst = $MgCO_3$; L = quenched liquid. High-temperature side is located at the right side of each image.

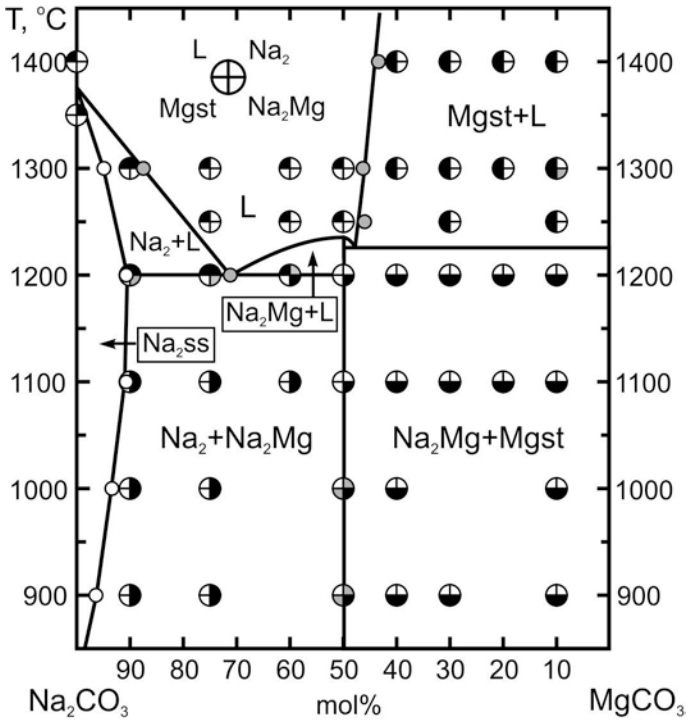

Figure 3. Phase relations in Na_2CO_3-$MgCO_3$ system at 6 GPa. Na_2ss = $MgCO_3$ solid solution in Na_2CO_3; Na_2Mg = $Na_2Mg(CO_3)_2$; Mgst = $MgCO_3$; L = liquid. Grey circles mark melt composition measured by EDS. Grey areas in the circles denote phases remaining in trace amount either due to kinetic problem, slight deviation of the system composition from $Na_2Mg(CO_3)_2$ stoichiometry or phases observed in the lower temperature side of partially molten samples.

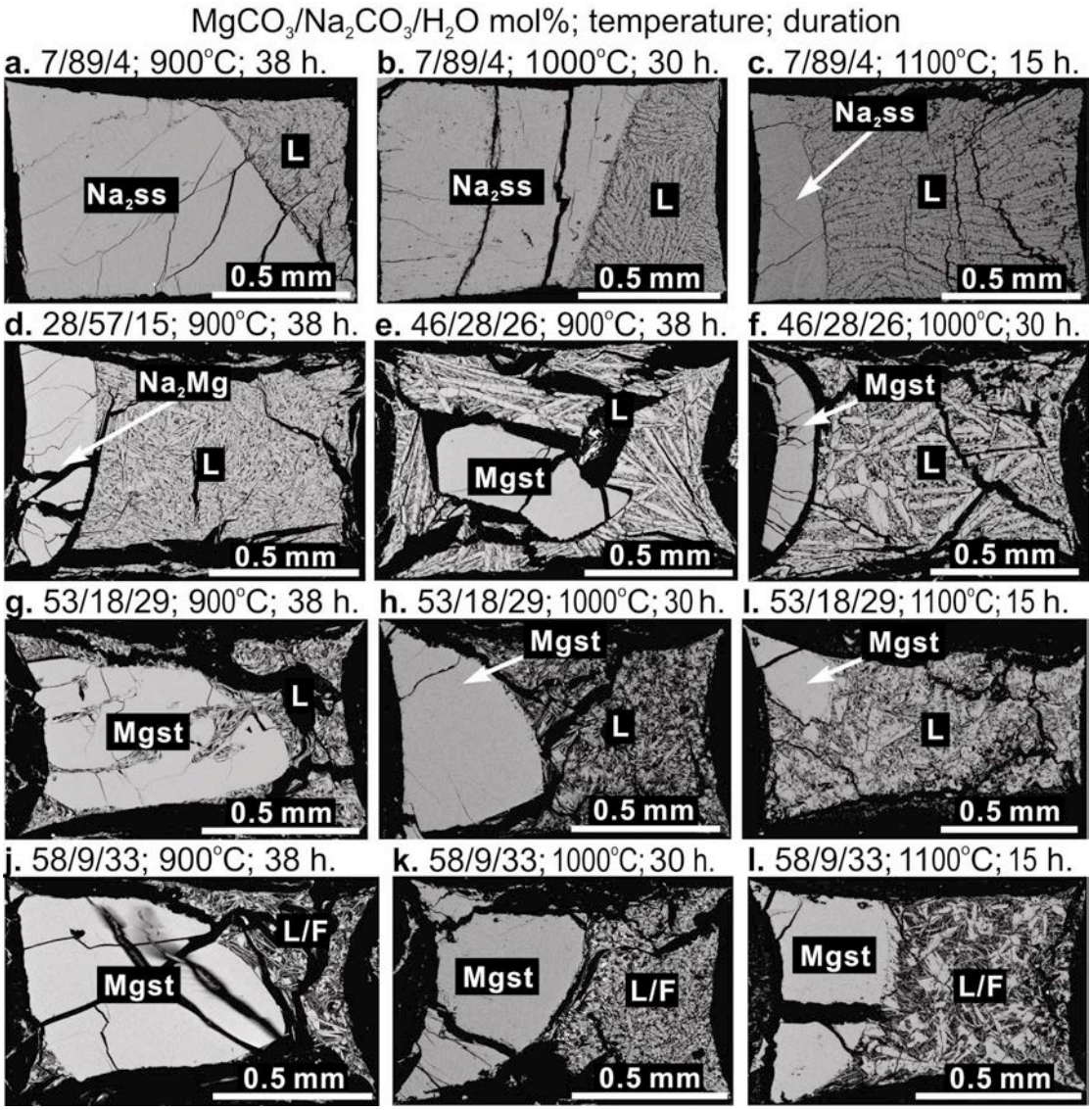

Figure 4. Representative BSE images of sample cross-sections illustrating phase relations in the systems Na_2CO_3-hydromagnesite at 6 GPa. Na_{2SS} = $MgCO_3$ solid-solutions in Na_2CO_3; Na_2Mg = $Na_2Mg(CO_3)_2$; Mgst = $MgCO_3$; L = quenched liquid or fluid. Gravity vector is directed from right to left in each image. The cassettes with samples were placed in the upper cassette of a BARS cell (Shatskiy et al. submitted to American Mineralogist # 4363). High-temperature side is located at the right side of each image.

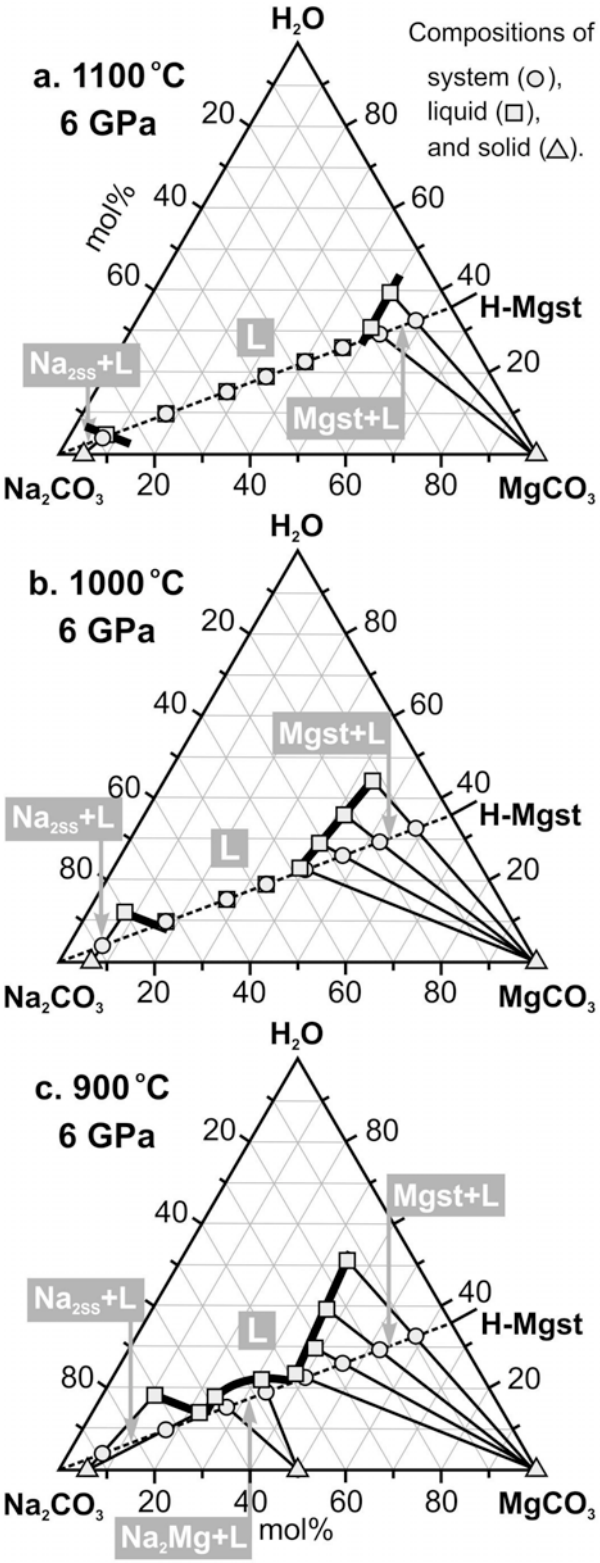

Figure 5. Triple diagrams illustrating the water effect on melting phase relations in the Na_2CO_3-$MgCO_3$ system at 6 GPa and 1100 °C (A), 1000 ºC (B), 900 ºC (C).

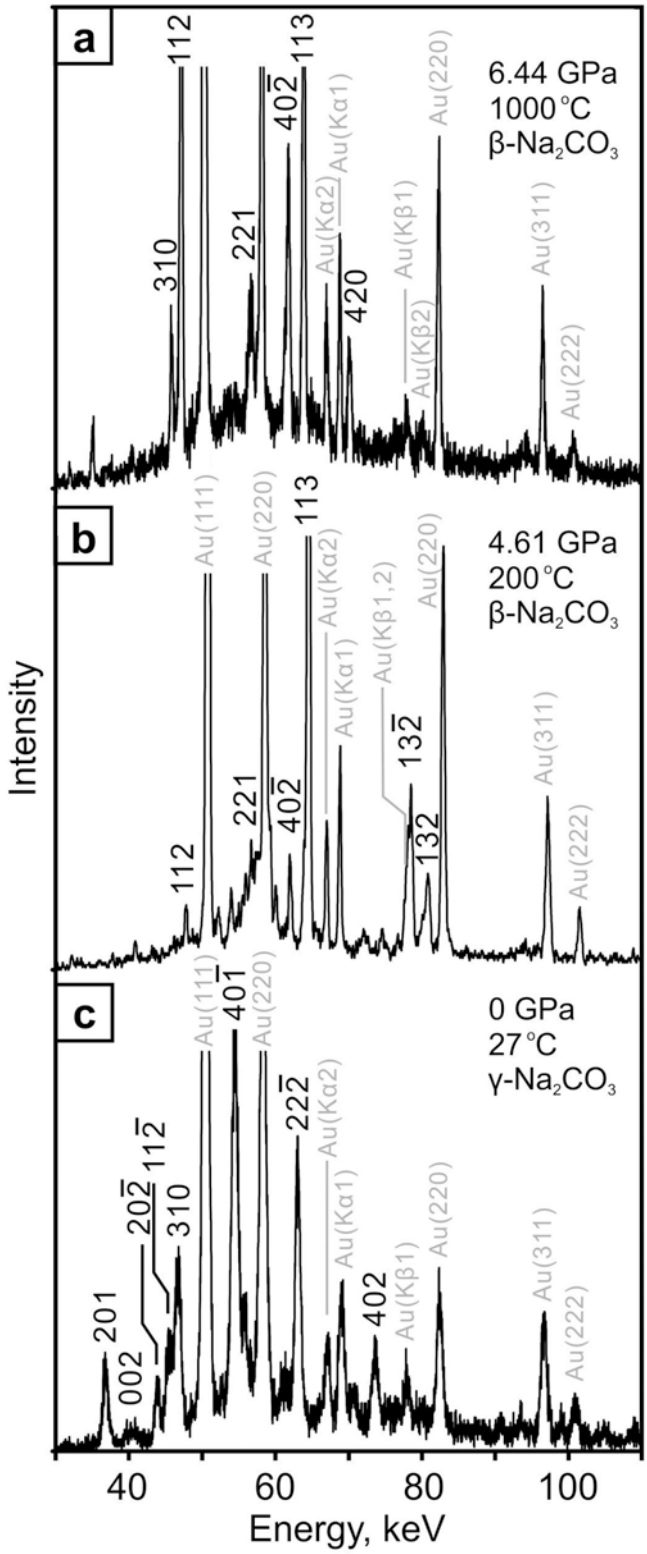

Figure 6. Representative energy dispersive X-ray diffraction patterns of β-Na_2CO_3 under HPHT conditions, run M1128 (A,B) and γ-Na_2CO_3 at ambient conditions after decompression, run M964 (C).

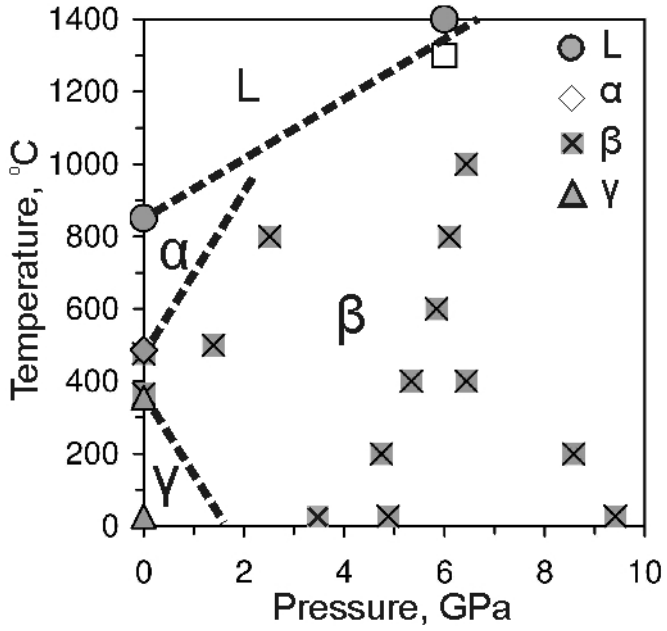

Figure 7. Pressure-temperature phase diagram of Na_2CO_3. The experimental data obtained using *in situ* X-ray diffraction and DIA-type multianvil apparatus at BL04B1 beamline SPring-8, runs M964 and M1128. High-temperature 1 atm data are from (Harris and Salje, 1992; Maciel and Ryan, 1981; Swainson et al., 1995). L is liquid. Open square is solid Na_2CO_3.

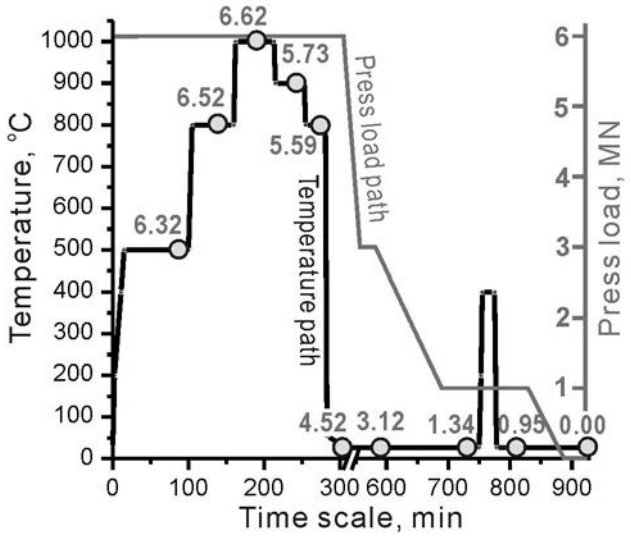

Figure 8. P-T pathway of the run M1250 on the *in situ* X-ray diffraction study of $Na_2Mg(CO_3)_2$. Grey circles with numbers above denote the conditions at which X-ray data from the sample were collected. Numbers denotes pressures using Au scale (Anderson et al., 1989).

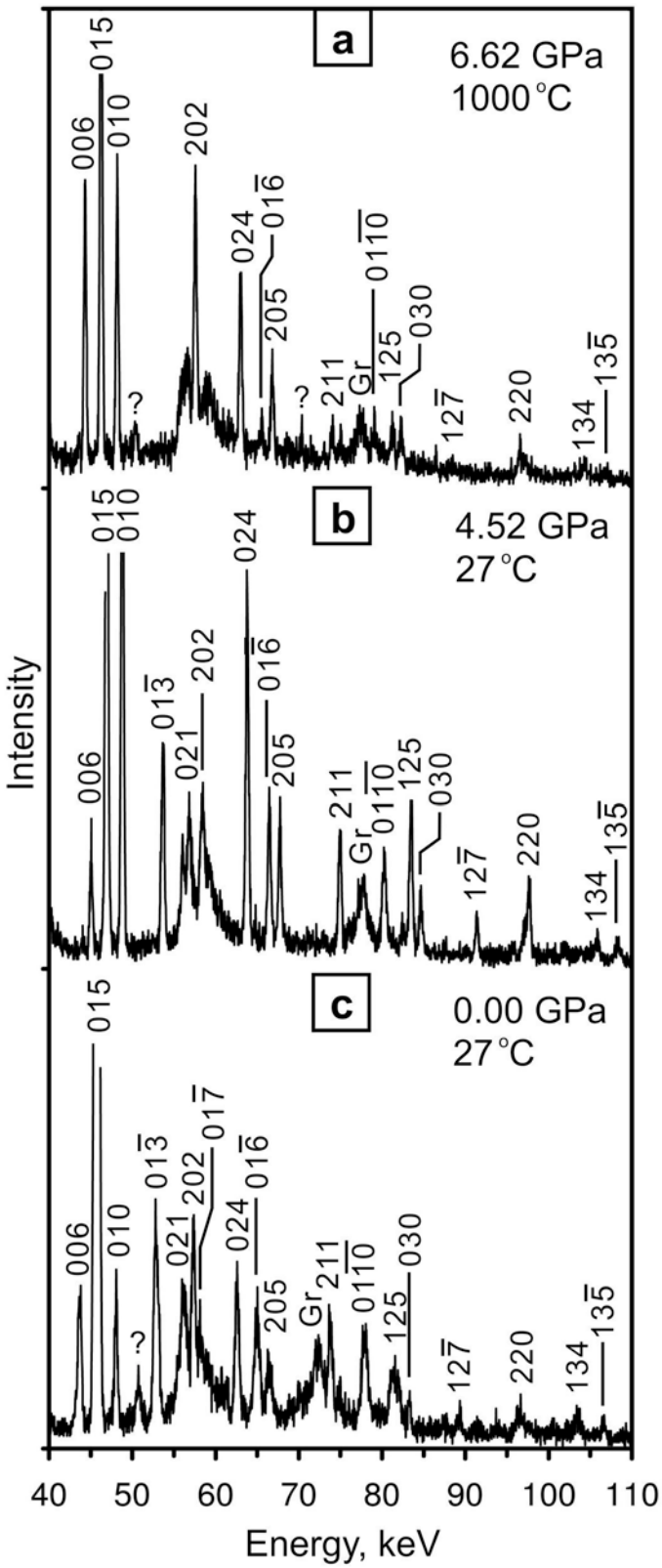

Figure 9. Representative energy dispersive X-ray diffraction profiles of eitelite, $Na_2Mg(CO_3)_2$, taken in the run M1250 under 6.6 GPa and 1000 °C (A), 4.5 GPa and 27 °C (B), and ambient conditions (C). Gr – graphite used as a sample capsule.

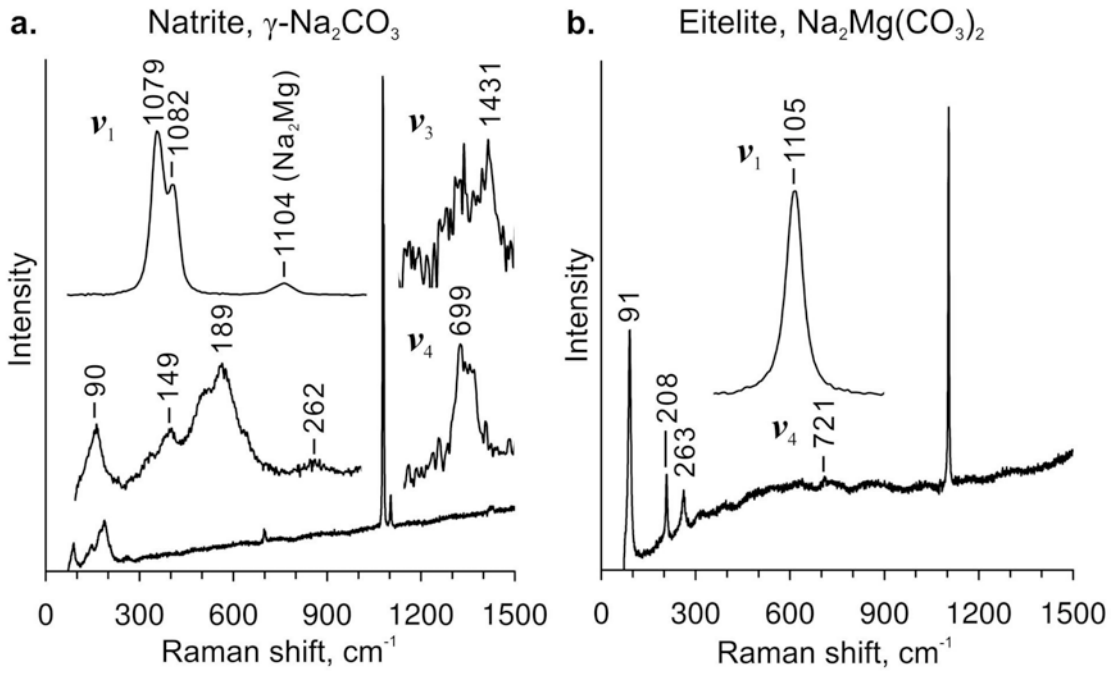

Figure 10. Representative unpolarized Raman spectra of γ-Na_2CO_3 (A) and $Na_2Mg(CO_3)_2$ (B) taken at ambient conditions in Ar atmosphere. The Raman measurements were made with an Ar^+ -ion laser working at 514 nm. Natrite was recovered from the system Na_2CO_3(90)-$MgCO_3$(10), run T2022 conducted at 6 GPa and 1100 ºC. Eitelite was synthesized in the system Na_2CO_3(50)-$MgCO_3$(50) at 6 GPa and 900 ºC, run T2021. The identifiers ν_n are referred to in (Meekes et al., 1986; White, 1974).

References cited

Akaishi, M., Kanda, H., and Yamaoka, S. (1990) Synthesis of diamond from graphite-carbonate systems under very high temperature and pressure. Journal of Crystal Growth, 104(2), 578-581.

Anderson, O.L., Isaak, D.G., and Yamamoto, S. (1989) Anharmonicity and the equation of state for gold. Journal of Applied Physics, 65(4), 1534-1543.

Brey, G.P., Bulatov, V.K., and Girnis, A.V. (2011) Melting of K-rich carbonated peridotite at 6-10 GPa and the stability of K-phases in the upper mantle. Chemical Geology, 281(3-4), 333-342.

Bulanova, G.P., and Pavlova, L.P. (1987) Magnesite peridotite assemblage in diamond from the Mir pipe. Doklady Akademii Nauk SSSR, 295(6), 1452-1456.

Buob, A., Luth, R.W., Schmidt, M.W., and Ulmer, P. (2006) Experiments on $CaCO_3$-$MgCO_3$ solid solutions at high pressure and temperature. American Mineralogist, 91, 435-440.

Cancarevic, Z., Schon, J.C., and Jansen, M. (2006) Alkali metal carbonates at high pressure. Zeitschrift Fur Anorganische Und Allgemeine Chemie, 632(8-9), 1437-1448.

Dalton, J.A., and Presnall, D.C. (1998) The continuum of primary carbonatitic-kimberlitic melt compositions in equilibrium with lherzolite: Data from the system CaO-MgO-Al2O3-SiO2-CO2 at 6 GPa. Journal of Petrology, 39(11-12), 1953-1964.

Dobrzhinetskaya, L.F., Green, H.W., Mitchell, T.E., and Dickerson, R.M. (2001) Metamorphic diamonds: Mechanism of growth and inclusion of oxides. Geology, 29(3), 263-266.

Dobrzhinetskaya, L.F., Wirth, R., and Green, H.W. (2006) Nanometric inclusions of carbonates in Kokchetav diamonds from Kazakhstan: A new constraint for the depth of metamorphic diamond crystallization. Earth and Planetary Science Letters, 243(1-2), 85-93.

Dusek, M., Chapuis, G., Meyer, M., and Petricek, V. (2003) Sodium carbonate revisited. Acta Crystallographica Section B-Structural Science, 59, 337-352.

Eitel, W., and Skaliks, W. (1929) Some double carbonates of alkali and earth alkali. Zeitschrift Fur Anorganische Und Allgemeine Chemie, 183(3), 263-286.

Fiquet, G., Guyot, F., Kunz, M., Matas, J., Andrault, D., and Hanfland, M. (2002) Structural refinements of magnesite at very high pressure. American Mineralogist, 87(8-9), 1261-1265.

Golovin, A.V., Sharygin, I.S., Korsakov, A.V., and Pokhilenko, N.P. (2012) Can parental kimberlite melts be alkali-carbonate liquids: Results of investigation of composition melt inclusions in the mantle xenoliths from kimberlites. 10th International Kimberlite Conference, p. 10IKC-91, Bangalore, India.

Grassi, D., and Schmidt, M.W. (2011) The melting of carbonated pelites from 70 to 700 km depth. Journal of Petrology, 52(4), 765-789.

Hammouda, T. (2003) High-pressure melting of carbonated eclogite and experimental constraints on carbon recycling and storage in the mantle. Earth and Planetary Science Letters, 214(1-2), 357-368.

Harris, M.J., and Salje, E.K.H. (1992) The incommensurate phase of sodium carbonate: an infrared absorption study. Journal of Physics-Condensed Matter, 4(18), 4399-4408.

Jamieson, J.C., Fritz, J.N., and Manghnani, M.H. (1982) Pressure measurement at high temperature in X-ray diffraction studies: gold as a primary standard. In S. Akimoto, and M.H. Manghnani, Eds. High pressure research in geophysics, p. 27-47. Center for Academic Publications, Tokyo.

Kamenetsky, V.S., Grutter, H., Kamenetsky, M.B., and Gomann, K. (2012) Parental carbonatitic melt of the Koala kimberlite (Canada): Constraints from melt inclusions in olivine and Cr-spinel, and groundmass carbonate. Chemical Geology, http://dx.doi.org/10.1016/j.chemgeo.2012.09.022.

Kamenetsky, V.S., Kamenetsky, M.B., Weiss, Y., Navon, O., Nielsen, T.F.D., and Mernagh, T.P. (2009) How unique is the Udachnaya-East kimberlite? Comparison with kimberlites from the Slave Craton (Canada) and SW Greenland. Lithos, 112, 334-346.

Kaminsky, F., Wirth, R., Matsyuk, S., Schreiber, A., and Thomas, R. (2009) Nyerereite and nahcolite inclusions in diamond: evidence for lower-mantle carbonatitic magmas. Mineralogical Magazine, 73(5), 797-816.

Kanda, H., Akaishi, M., and Yamaoka, S. (1990) Morphology of synthetic diamonds grown from Na_2CO_3 solvent-catalyst. Journal of Crystal Growth, 106(2-3), 471-475.

Katsura, T., and Ito, E. (1990) Melting and subsolidus relations in the $MgSiO_3$–$MgCO_3$ system at high pressures: implications to evolution of the Earth's atmosphere. Earth and Planetary Science Letters, 99, 110–117.

Katsura, T., Tsuchida, Y., Ito, E., Yagi, T., Utsumi, W., and Akimoto, S. (1991) Stability of magnesite under lower mantle conditions. Proceedings of the Japan Academy Series B-Physical and Biological Sciences, 67(4), 57-60.

Kavanagh, J.L., and Sparks, R.S.J. (2009) Temperature changes in ascending kimberlite magma. Earth and Planetary Science Letters, 286(3-4), 404-413.

Kennedy, C.S., and Kennedy, G.C. (1976) The equilibrium boundary between graphite and diamond. Journal of Geophysical Research, 81(14), 2467-2470.

Klein-BenDavid, O., Izraeli, E.S., Hauri, E., and Navon, O. (2004) Mantle fluid evolution - a tale of one diamond. Lithos, 77(1-4), 243-253.

-. (2007) Fluid inclusions in diamonds from the Diavik mine, Canada and the evolution of diamond-forming fluids. Geochimica Et Cosmochimica Acta, 71(3), 723-744.

Klein-BenDavid, O., Logvinova, A.M., Schrauder, M., Spetius, Z.V., Weiss, Y., Hauri, E.H., Kaminsky, F.V., Sobolev, N.V., and Navon, O. (2009) High-Mg carbonatitic microinclusions in some Yakutian diamonds - a new type of diamond-forming fluid. Lithos, 112, 648-659.

Korsakov, A.V., Golovin, A.V., De Gussem, K., Sharygin, I.S., and Vandenabeele, P. (2009) First finding of burkeite in melt inclusions in olivine from sheared lherzolite xenoliths. Spectrochimica Acta Part A: Molecular and Biomolecular Spectroscopy, 73(3), 424-427.

Litasov, K.D., Fei, Y.W., Ohtani, E., Kuribayashi, T., and Funakoshi, K. (2008) Thermal equation of state of magnesite to 32 GPa and 2073 K. Physics of the Earth and Planetary Interiors, 168(3-4), 191-203.

Litasov, K.D., and Ohtani, E. (2010) The solidus of carbonated eclogite in the system CaO-Al_2O_3-MgO-SiO_2-Na_2O-CO_2 to 32 GPa and carbonatite liquid in the deep mantle. Earth and Planetary Science Letters, 295, 115-126.

Litasov, K.D., Sharygin, I.S., Shatskiy, A.F., Ohtani, E., and Pokhilenko, N.P. (2010) Experimental constraints on the role of chloride in the origin and evolution of kimberlitic magma. Doklady Earth Sciences, 435(2), 1641-1646.

Litasov, K.D., Shatskiy, A., Ohtani, E., and Yaxley, G.M. (2013) The solidus of alkaline carbonatite in the deep mantle. Geology, 41(1), 79-82.

Luth, R.W. (2006) Experimental study of the $CaMgSi_2O_6$-CO_2 system at 3-8 GPa. Contributions to Mineralogy and Petrology, 151(2), 141-157.

Maciel, A., and Ryan, J.F. (1981) Observation of coupled amplitude modes in the Raman spectrum of incommensurate Na_2CO_3. Journal of Physics C-Solid State Physics, 14(18), L509-L514.

McKie, D. (1990) Subsolidus phase relations in the system $K_2Ca(CO_3)_2$-$Na_2Mg(CO_3)_2$ at 1 kbar: The fairchildite$_{ss}$-buetschliite-eitelite eutectoid. American Mineralogist, 75(9-10), 1147-1150.

Meekes, H., Rasing, T., Wyder, P., Janner, A., and Janssen, T. (1986) Raman and infrared spectra of the incommensurate crystal Na_2CO_3. Physical Review B, 34(6), 4240-4254.

Mitchell, R.H., and Kjarsgaard, B.A. (2011) Experimental studies of the system Na_2CO_3-$CaCO_3$-MgF_2 at 0-1 GPa: Implications for the differentiation and low-temperature crystallization of natrocarbonatite. Journal of Petrology, 52(7-8), 1265-1280.

Navon, O. (1991) High internal pressure in diamond fluid inclusions determined by infrared absorption. Nature, 353(6346), 746-748.

Pabst, A. (1973) The crystallography and structure of eitelite, $Na_2Mg(CO_3)_2$. American Mineralogist, 58(3-4), 211-217.

Pal'yanov, Y.N., Sokol, A.G., Borzdov, Y.M., and Khokhryakov, A.F. (2002) Fluid-bearing alkaline carbonate melts as the medium for the formation of diamonds in the Earth's mantle: an experimental study. Lithos, 60(3-4), 145-159.

Pal'yanov, Y.N., Sokol, A.G., Borzdov, Y.M., Khokhryakov, A.F., Shatsky, A.F., and Sobolev, N.V. (1999a) The diamond growth from Li_2CO_3, Na_2CO_3, K_2CO_3 and Cs_2CO_3 solvent-catalysts at P=7 GPa and T=1700-1750 ^oC. Diamond and Related Materials, 8(6), 1118-1124.

Pal'yanov, Y.N., Sokol, A.G., Borzdov, Y.M., Khokhryakov, A.F., and Sobolev, N.V. (1999b) Diamond formation from mantle carbonate fluids. Nature, 400(6743), 417-418.

Palyanov, Y.N., Borzdov, Y.M., Khokhryakov, A.F., Kupriyanov, I.N., and Sokol, A.G. (2010) Effect of nitrogen impurity on diamond crystal growth processes. Crystal Growth & Design, 10(7), 3169-3175.

Schrauder, M., and Navon, O. (1994) Hydrous and carbonatitic mantle fluids in fibrous diamonds from Jwaneng, Botswana. Geochimica Et Cosmochimica Acta, 58(2), 761-771.

Seto, Y., Hamane, D., Nagai, T., and Fujino, K. (2008) Fate of carbonates within oceanic plates subducted to the lower mantle, and a possible mechanism of diamond formation. Physics and Chemistry of Minerals, 35(4), 223-229.

Sharygin, I.S., Korsakov, A.V., Golovin, A.V., and Pokhilenko, N.P. (Accepted) Eitelite from Udachanya-East kimberlite pipe (Russia) – A new locality and host rock type. European Journal of Mineralogy.

Sharygin, I.S., Litasov, K.D., Shatskiy, A.F., Golovin, A.V., Ohtani, E., and Pokhilenko, N.P. (2013) Melting of kimberlite of the Udachnaya East pipe: experimental study at 3–6.5 GPa and 900–1500°C. Doklady Earth Sciences, 448, 200-205.

Shatskii, A.F., Borzdov, Y.M., Sokol, A.G., and Pal'yanov, Y.N. (2002) Phase formation and diamond crystallization in carbon-bearing ultrapotassic carbonate-silicate systems. Geologiya I Geofizika, 43(10), 940-950.

Shatskiy, A., Borzdov, Y.M., Litasov, K.D., Ohtani, E., Khokhryakov, A.F., Palyanov, Y.N., and Katsura, T. (2011) Pressless split-sphere apparatus equipped with scaled-up Kawai-cell for mineralogical studies at 10-20 GPa. American Mineralogist, 96, 541-548.

Shatskiy, A., Borzdov, Y.M., Sharygin, I.S., Litasov, K.D., and N., P.Y. (Under review-a) The system K_2CO_3-$CaCO_3$ at 6 GPa and 900-1400 ºC. American Mineralogist.

Shatskiy, A., Sharygin, I.S., Gavryushkin, P.N., Litasov, K.D., Borzdov, Y.M., Shcherbakova, A.V., Higo, Y., and Funakoshi, K. (Accepted) The system K_2CO_3-$MgCO_3$ at 6 GPa and 900-1450 ºC. American Mineralogist.

Shatskiy, A., Sharygin, I.S., Litasov, K.D., Borzdov, Y.M., and Ohtani, E. (Under review-b) The system Na_2CO_3-$CaCO_3$ at 6 GPa and 900-1400 ºC. American Mineralogist.

Shatsky, V.S., Ragozin, A.L., and Sobolev, N.V. (2006) Some aspects of metamorphic evolution of ultrahigh-pressure calc-silicate rocks of the Kokchetav Massif. Russian Geology and Geophysics, 47(1), 105-119.

Smith, E.M., Kopylova, M.G., Dubrovinsky, L., Navon, O., Ryder, J., and Tomlinson, E.L. (2011) Transmission X-ray diffraction as a new tool for diamond fluid inclusion studies. Mineralogical Magazine, 75(5), 2657-2675.

Sobolev, N.V., and Shatsky, V.S. (1990) Diamond inclusions in garnets from metamorfic rocks: a new environment for diamond formation. Nature, 343(6260), 742-746.

Sokol, A.G., Pal'yanov, Y.N., Borzdov, Y.M., Khokhryakov, A.F., and Sobolev, N.V. (1998) Crystallization of diamond from Na_2CO_3 melt. Doklady Akademii Nauk, 361(3), 388-391.

Sokol, A.G., Palyanov, Y.N., and Surovtsev, N.V. (2007) Incongruent melting of gallium nitride at 7.5 GPa. Diamond and Related Materials, 16(3), 431-434.

Swainson, I.P., Dove, M.T., and Harris, M.J. (1995) Neutron powder diffraction study of the ferroelastic phase transition and lattice melting in sodium carbonate, Na_2CO_3. Journal of Physics-Condensed Matter, 7(23), 4395-4417.

Tomlinson, E.L., Jones, A.P., and Harris, J.W. (2006) Co-existing fluid and silicate inclusions in mantle diamond. Earth and Planetary Science Letters, 250(3-4), 581-595.

Wang, A., Pasteris, J.D., Meyer, H.O.A., and DeleDuboi, M.L. (1996) Magnesite-bearing inclusion assemblage in natural diamond. Earth and Planetary Science Letters, 141(1-4), 293-306.

Weiss, Y., Kessel, R., Griffin, W.L., Kiflawi, I., Klein-BenDavid, O., Bell, D.R., Harris, J.W., and Navon, O. (2009) A new model for the evolution of diamond-forming fluids: Evidence from microinclusion-bearing diamonds from Kankan, Guinea. Lithos, 112, 660-674.

White, W.B. (1974) The carbonate minerals. In V.C. Farmer, Ed. The Infrared Spectra of the Minerals, Mineralogical Society Monograph, p. 227-284. Mineralogical Society, London.

Zedgenizov, D.A., Kagi, H., Shatsky, V.S., and Sobolev, N.V. (2004) Carbonatitic melts in cuboid diamonds from Udachnaya kimberlite pipe (Yakutia): evidence from vibrational spectroscopy. Mineralogical Magazine, 68(1), 61-73.

Zedgenizov, D.A., Ragozin, A.L., Shatsky, V.S., Araujo, D., and Griffin, W.L. (2011) Fibrous diamonds from the placers of the northeastern Siberian Platform: carbonate and silicate crystallization media. Russian Geology and Geophysics, 52(11), 1298-1309.

Zedgenizov, D.A., Rege, S., Griffin, W.L., Kagi, H., and Shatsky, V.S. (2007) Composition of trapped fluids in cuboid fibrous diamonds from the Udachnaya kimberlite: LAM-ICPMS analysis. Chemical Geology, 240(1-2), 151-162.